CONTRAST MEDIA & MOLECULAR IMAGING

Received: 9 February 2012, Revised: 4 May 2012, Accepted: 14 June 2012, Published online in Wiley Online Library: 2012

(wileyonlinelibrary.com) DOI: 10.1002/cmmi.1482

Two forms of iron as an intrinsic contrast agent in the basal ganglia of PKAN patients

Monika Dezortova[a]*, Vit Herynek[a], Martin Krssak[b,c], Claudia Kronerwetter[b], Siegfried Trattnig[b] and Milan Hajek[a]

Iron deposits in the human brain can be considered as intrinsic contrast agents for magnetic resonance imaging and are used as markers of neurodegeneration accompanied by brain-iron accumulation. We studied one of them – panthotenate-kinase associated neurodegeneration (PKAN) – by using relaxometry at 1.5, 3.0 and 7 T in a group of six patients; we also measured a group of five volunteers for comparison. Based on the magnetic field dependency of antiferromagnetic ferritin and maghemite iron oxide nanoparticle relaxivities, we derived a two-component model for the description of iron deposits in the globus pallidus of PKAN patients. According to this model, we estimated the iron content in PKAN patients as 391 μg/ml of antiferromagnetic iron (ferritin) and 1.1 μg/ml of ferrimagnetic iron, compared with 178 μg/ml of iron in ferritin found in controls. This two-component model explains the nonlinear shape of the relaxometric curves in *in vivo* measurements of the relaxation rates of PKAN patients and is supported by histological findings in the original reports on PKAN patients. Copyright © 2012 John Wiley & Sons, Ltd.

Keywords: MR relaxometry; basal ganglia; PKAN; iron deposits; ferritin; SPIO

1. INTRODUCTION

Iron ions play an important role in a number of key metabolic pathways in the human body. In the healthy brain, non-hemic iron begins to deposit shortly after birth, and its concentration increases with age (1). Iron accumulation is most pronounced in the globus pallidus, where it starts approximately at the age of 6 months. Between the months 9 and 12, iron begins to be deposited in the zona reticulate of the substantia nigra. However, an excess of iron deposits leads to severe diseases classified as neurodegeneration accompanied by brain-iron accumulation (NBIA). The magnetic properties of iron complexes make them indirectly observable in magnetic resonance (MR) images, and these compounds can be considered as intrinsic contrast agents.

Irreversible iron accumulation is a sign of a rare autosomal-recessive disorder, the so-called panthotenate-kinase associated neurodegeneration (PKAN, formerly known as the Hallervorden–Spatz syndrome) (2). PKAN affects both genders and is caused by a mutation in the gene encoding pantothenate kinase 2 (PANK2). It affects the biochemical pathway of vitamin B5 (pantothenate acid) and results in an increasing amount of iron in some parts of the basal ganglia (globus pallidus and substantia nigra).

Characteristic MR findings in PKAN patients include hypointense regions in the globus pallidus (GP) and substantia nigra, mostly accompanied by hyperintensity in the anterio-medial part of the globus pallidus described as an 'eye-of-the-tiger' sign. However, the hyperintensity may not occur in all patients with a positive genetically confirmed diagnosis (e.g. in our patient P3). Its presence is explained by gliotic changes and an edema, whereas iron is accumulated in the hypointensive rim of the GP (2,3).

Magnetic resonance relaxometry not only detects the simple presence of iron (and other paramagnetic substances) deposits, but it may also enable the estimation of iron concentration and its form (4). Non-hemic iron is deposited in the body, especially in the form of the water-soluble intracellular protein ferritin. The ferritin molecule has a hollow spherical shape and traps ferrous ions, oxidizes them to ferric ions and stores them inside in the form of an antiferromagnetic ferrihydrite crystal. Each molecule can store up to 4500 iron ions. Thus, it protects cells from divalent iron toxicity. Experiments have suggested that ferritin T_2 relaxivity linearly increases with an increasing magnetic field, while the slope depends on the ferritin loading factor, i.e. the amount of iron ions inside (5–7). The results of *in vitro* measurements on fixed samples indicated a quadratic dependence of the relaxation rate on the magnetic field in the brain nuclei (8). One of the explanations could be the tissue-specific behavior of ferritin relaxivity, while another could be the presence of different iron complexes in the brain tissue manifested by different magnetic properties. Even a crystal inside the ferritin may not be completely antiferromagnetic, as there might be a layer of disordered ions on its surface resulting in partially ferro- or ferrimagnetic properties (9). In the case of excessive iron deposits, we may expect a higher ratio of disordered ions on the iron core of the ferritin, or even the

* *Correspondence to: M. Dezortova, MR Unit, Department of Diagnostic and Interventional Radiology, Institute for Clinical and Experimental Medicine, Videnska 1958/9, 140 21 Prague 4, Czech Republic. Email: mode@medicon.cz*

a *M. Dezortova, V. Herynek, M. Hajek*
MR Unit, Department of Diagnostic and Interventional Radiology, Institute for Clinical and Experimental Medicine, Prague, Czech Republic

b *M. Krssak, C. Kronerwetter, S. Trattnig*
MR Centre of Excellence, Department of Radiology, Medical University of Vienna, Vienna, Austria

c *M. Krssak*
Division of Endocrinology and Metabolism, Department of Internal Medicine III., Medical University of Vienna, Vienna, Austria

presence of iron with stronger superparamagnetic properties of a different origin. The latter hypothesis can be also supported by the original findings of Hallervorden and Spatz (10), who proposed two different iron compartments based on the Prussian-blue staining of brain samples from a PKAN patient. Ferrimagnetic iron can be represented by maghemite nanoparticles (in the literature known as superparamagnetic iron oxide nanoparticles, SPIO) that may be identified owing to substantially shortened T_2 and T_2* relaxation times. Therefore, they were used as MR contrast agents and now are broadly used in cellular and molecular imaging as a cellular marker (11,12). As a result of different iron bonds and the ferrimagnetic character of these nanoparticles compared with ferritin, a small amount of SPIO can significantly increase transverse relaxivity.

In our previous study we described a one-component model characterizing iron deposits in the globus pallidus of PKAN patients in the form of ferritin only (13). The goal of the present study was to measure the iron load of the brain tissue in PKAN patients and to identify different forms of iron in order to estimate their possible contribution to the deposits based on relaxation times measured at different magnetic fields and by comparison to controls and phantoms containing different forms of iron.

2. RESULTS

Characteristic MRI hypointensive lesions in the globus pallidus and substantia nigra were observed in all patients in the used magnetic fields. Also, the 'eye-of-the-tiger' sign (i.e. a hypointense GP with a hyperintense medial part) of various size, intensity and shape was observed in the patients (with the exception of patient P3). T_2-weighted transversal MR images through the basal ganglia of the PKAN patients and the healthy volunteers are shown in Fig. 1.

As we did not observe any significant differences between the left and right hemispheres (no significant difference shown by a *t*-test), we pooled the data from both hemispheres. Also, no statistical difference was found between the three evaluators; therefore, we pooled the data, and Table 1 summarizes the mean T_2 values for each selected area and each magnetic field.

We found significantly decreased T_2 relaxation times in the GP (corresponding to the hypointense lesions in MR images) in all the patients compared with the controls in all the used magnetic fields. Interestingly, a statistically significant increase ($p < 0.05$) in T_2 relaxation times was found in the putamen and caudate nucleus in the patients compared with the controls (Table 1).

Iron concentrations were calculated from the T_2 values according to the empirical equation (1) derived in Hajek *et al*. (13) and based on the published values of iron concentration in the brain (1) and normal T_2 (14). The calculated concentrations of iron in the globus pallidus in the controls examined at 1.5 T corresponded to the presumed normal iron concentration assessed by Hallgren and Sourander (1). In patients, the one-component model revealed iron concentrations that were more than double those found in the controls (13) (Table 2, Fig. 2).

The field dependences of relaxation rates R_2 at 1. 5–7 T in the evaluated brain areas, with the exception of the GP, showed a similar convex shape of the curves in both the patients and the controls (Fig. 3). In contrast, the relaxation rates in the globus pallidus of the patients followed a concave shape.

In the phantoms, the field dependences of the r_2 relaxivity of ferritin and SPIO at 0.5–7 T were different (Fig. 4). Ferritin solutions revealed an almost linear increase of r_2 with the magnetic field B_0 (5–7,15), while SPIO nanoparticles showed more or less constant relaxivity values in different magnetic fields (Fig. 4). The measured relaxivities of ferritin and SPIO were used to calculate iron concentrations in the GP in patients using a two-component model.

Further evaluation was based on the assumption that the relaxations in the phantoms and in the brain tissue are similar. Assuming that the contribution of the surplus iron to the relaxation rate can be described as the difference between the relaxation rates of PKAN patients and healthy controls, we estimated the proportional content of both iron components. The best approximation to the patients' surplus iron content was 213 μg/ml of iron in an

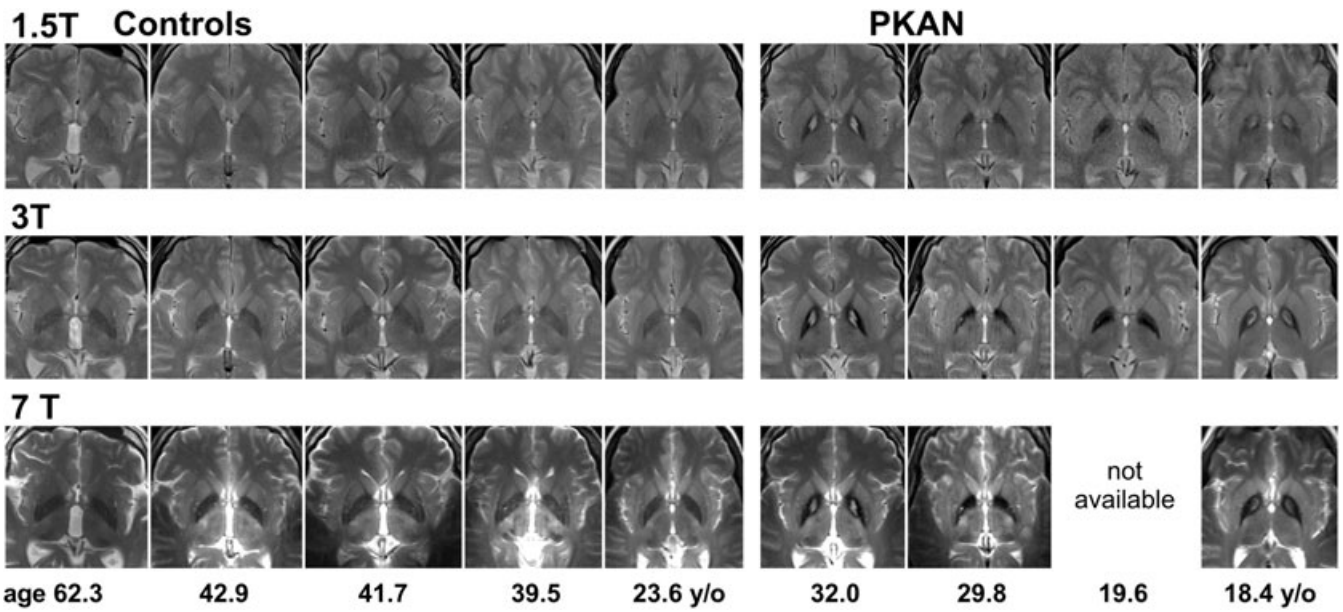

Figure 1. T_2-weighted images of PKAN patients and controls obtained in three different magnetic fields arranged by decreasing age (1.5 and 3 T, *TR*/*TE* = 3000/75.9 ms; 7 T, *TR*/*TE* = 6000/75.9 ms).

Table 1. T_2 relaxation times (ms; mean ± standard deviation) in the globus pallidus (or in its dark rim part; Fig. 5) together with other parts of the basal ganglia and frontal white matter obtained in different magnetic fields. For comparison, individual patient data are also shown

Brain area	B_0	Controls, $N=5$	Patients, $N=3$	Patient P1	Patient P2	Patient P4
Globus pallidus	1.5 T	69.1 ± 1.5	51.8 ± 4.9 ↓	48.8	48.2	58.3
	3 T	55.8 ± 1.7	36.4 ± 3.8 ↓	35.2	33.2	40.8
	7 T	31.9 ± 1.4	23.2 ± 2.4 ↓	23.2	20.9	25.5
Putamen	1.5 T	81.3 ± 2.0	85.5 ± 3.5 ↑	85.7	81.7	89.1
	3 T	70.8 ± 3.0	75.7 ± 2.8 ↑	73.8	73.8	79.4
	7 T	44.5 ± 2.8	48.7 ± 3.2 ↑	47.6	45.8	52.8
Nucleus caudatus	1.5 T	90.6 ± 2.5	94.5 ± 4.3 ↑	98.1	88.9	96.6
	3 T	80.3 ± 2.5	86.1 ± 1.8 ↑	85.5	84.8	88.1
	7 T	52.6 ± 2.3	57.0 ± 1.6 ↑	57.9	55.3	57.9
White matter	1.5 T	74.1 ± 1.2	73.4 ± 2.4	74.3	70.6	75.3
	3 T	69.8 ± 1.7	69.0 ± 0.5	69.0	69.2	68.8
	7 T	50.6 ± 1.0	49.3 ± 1.0	50.0	48.2	49.7

↓,↑ Indicate significant differences ($p < 0.001$) between patient and control groups.

Table 2. Fe concentrations (μg/ml) calculated using T_2 relaxation times (ms) obtained at 1.5 T in the globus pallidus (alternatively in its dark rim only). In patients, one-component (ferritin only) and two-component (ferritin + SPIO) models were used

Controls	C1	C2	C3	C4	C5			Mean ± SD
Age (years)	62.3	42.9	41.7	39.5	23.6			—
T_2 (ms)	66.8	68.8	69.7	70.7	69.3			69.1 ± 1.5
Fe concentration (μg/ml)	196	180	173	165	176			177.8 ± 10.2
Patients	**P1**	**P2**	**P3**	**P4**	**P5**	**P6**	**P3**	
Age (years)	32.0	29.8	19.6	18.4	15.5	14.2	13.8	—
T_2 (ms)	48.8	48.2	39.5	58.3	42.3	45.8	44.7	46.8
One-component model:								
Fe concentration in ferritin form (μg/ml)	400	409	578	276	517	450	470	443
Two-component model:								
Total Fe concentration in ferritin (μg/ml)	343.6	351.0	477.8	254.1	433.1	380.9	395.8	391.3
in SPIO[a] (μg/ml)	0.85	0.89	1.55	0.39	1.32	1.05	1.12	1.1

[a]SPIO is Endorem® in our case.

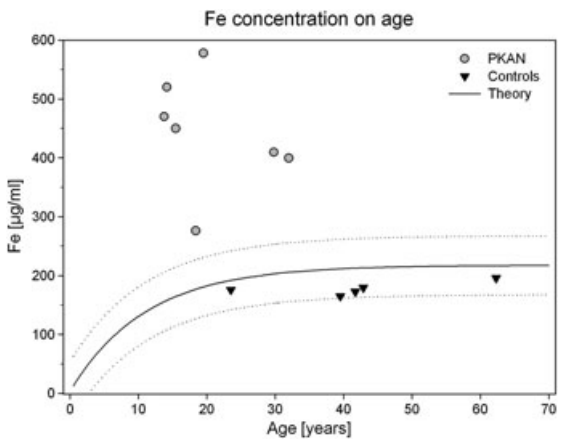

Figure 2. Relation between iron deposition in the globus pallidus and age. Iron concentration was calculated using a one-component model. The theoretical curve was calculated based on Hallgren and Sourander's data (1): circles, patients; triangles, healthy controls.

antiferromagnetic form and 1.1 μg/ml of iron in a ferrimagnetic form. Thus, the total amount of iron in the GP of our PKAN group was around 391 μg/ml of iron in the form of ferritin (including physiological ferritin) and 1.1 μg/ml of ferrimagnetic iron with strong superparamagnetic properties.

Interestingly, owing to its high relaxivity, even a small portion (0.05–0.3%) of the ferrimagnetic form of iron substantially increased the relaxation rate. Iron concentration in the globus pallidus evaluated according to this model is shown in Table 2.

3. DISCUSSION

The 'eye-of-the-tiger' sign is well known and has been already described, as well as the hypointense signal, in the globus pallidus observable in T_2-weighted images (2,13,16). The contrast between the hyperintense center and the hypointense rim increases with the magnetic field (Fig. 1). Hypointensity in PKAN patients corresponds to a shortened T_2 relaxation time caused by iron deposits. The form of iron deposits in the basal ganglia of

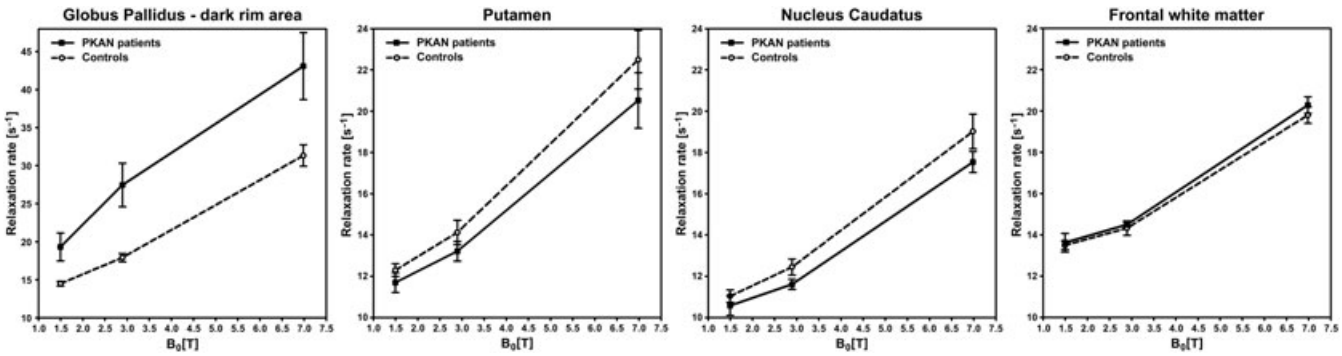

Figure 3. Dependence of relaxation rates ($R_2 = 1/T_2$) on B_0 in different parts of the brain. The graphs show the average patient (solid line) and control (dashed line) data.

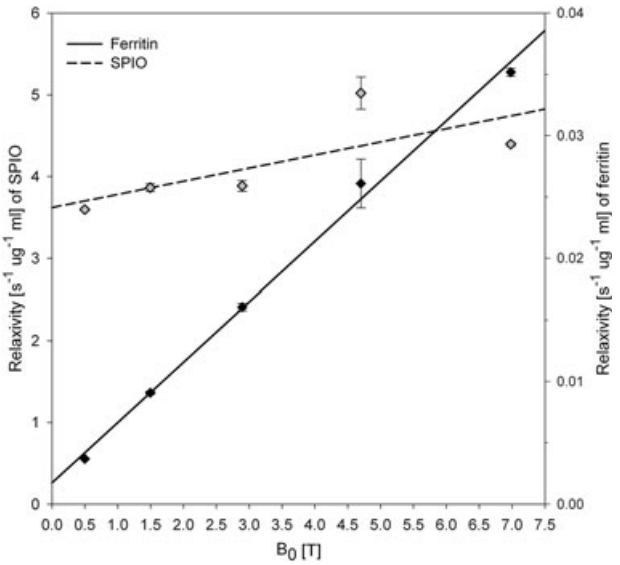

Figure 4. Dependence of relaxivities r_2 on B_0 in phantoms containing ferritin and SPIO contrast media: solid line, ferritin; dashed line, SPIO.

PKAN patients is unclear. In healthy subjects, iron in the brain is predominantly present in the form of ferritin, which prevents oxidative stress by oxidizing divalent Fe^{2+} to Fe^{3+} ions that are subsequently stored inside the apoferritin as antiferromagnetic crystals. Oxidized iron cannot enter the Fenton reaction, which would lead to the formation of free radicals. So far, the generally accepted explanation for the pathological changes in PKAN patients involves an increased iron concentration in the form of ferritin.

Assuming that all iron deposits are in the form of ferritin, the iron concentration can be easily calculated from the relaxation time according to eqn (1) (13). The concentrations of iron would be in the range of 280–580 μg/ml (Table 2) in the patients and 180 μg/ml in the controls (which is in line with published data (1,13,14)). However, differences in the field dependency of the relaxation rates (Fig. 3) indicate that the assumption that iron is deposited only in ferritin in an antiferromagnetic form may not be correct.

As early as in 1922, Hallervorden and Spatz (10) pointed out that iron in the brain might be present in different forms. If iron in the brain of PKAN patients is deposited in different forms, we can also expect different magnetic properties. Besides antiferromagnetic iron in ferritin molecules, ferrimagnetic iron (as a magnetite or maghemite) might also be present. This would substantially change the effect of iron on the relaxation times. Examination of the subjects in different field strengths helped to identify the form of these deposits in the brain.

The field dependence of the relaxation rates in the group of controls revealed a similar trend as described for the *in vitro* examination of brain nuclei samples obtained from old brain donors with no neurodegenerative diseases (8). A similar behavior was observed in the basal ganglia of the PKAN patients with the exception of the GP (Fig. 3).

The relaxation rates in the GP of PKAN patients differ from those of the controls not only in their magnitude, but also in the shape of the field dependence. This fact supports the hypothesis that iron is also deposited in other forms than in ferritin. Therefore, we used a model anticipating the presence of both antiferromagnetic (ferritin) and ferrimagnetic (SPIO) iron for the estimation of iron concentration. The calculated amount of ferrimagnetic iron is very small compared with antiferromagnetic iron; nevertheless, its impact on the relaxation rate is substantial owing to strong superparamagnetic effect.

Although the calculation of iron concentrations using the two-component model has to be considered as an estimation only, it confirms the presence of at least two forms of iron in the basal ganglia of PKAN patients. This result also supports earlier histological findings (i.e. staining for Prussian blue (10) and electron microscopy (17,18) findings).

Nevertheless, the origin of the second component remains unknown. We cannot exclude even iron microcrystals from hemosiderin or denaturated ferritin (which would explain the staining for Prussian Blue) or some other effect (9).

Contrary to the shortening of the T_2 relaxation time in the GP, an increase in T_2 relaxation times in the putamen and nucleus caudate in patients is a new finding. Although these differences are rather slight, their statistical significance ($p < 0.001$) was proved in all three magnetic fields, and thus they should not be disregarded. We have not found any information in the literature confirming or disproving our findings, and we do not have, at the moment, a clear explanation for this effect.

We found no correlation between the first clinical symptoms of the disease and the calculated iron concentration. In patient P4, a deviation in iron concentration from the other patients' data (Fig. 2) was observed. Measurements at both 3 and 7 T confirmed this tendency; therefore, we can exclude an experimental error. Genetic differences might be responsible for such differences; nevertheless, the same mutation in homogeneous form was also found in patient P1. The other patients (except for patient P2) have this mutation heterozygously (Table 3).

Table 3. Patient description

Subject	Sex, age (years)	Mutation[a]	MR examination
P1	M, 32.0	c.1583C > T (p.Thr528Met) in exon 6 of gene PANK2 – homozygous	1.5 T, 3 T, 7 T
P2	F, 29.8	c.1369G > T (p.Asp457Tyr) in exon 4 of gene PANK2 – heterozygous c.1561G > A (p.Gly521Arg) in exon 6 of gene PANK2 – heterozygous	1.5 T, 3 T, 7 T
P3	F, 13.8 and 19.6	c.1583C > T (p.Thr528Met) in exon 6 of gene PANK2 – heterozygous c.1235 + 5G > A in intron 3 of gene PANK2 – heterozygous c.1413-8_1413-9dupTTCCCC in intron 4 of gene PANK2 – heterozygous	1.5 T repeatedly, 3 T
P4	F, 18.4	c.1583C > T (p.Thr528Met) in exon 6 of gene PANK2 – homozygous	1.5 T, 3 T, 7 T
P5	M,15.5	c.1583C > T (p.Thr528Met) in exon 6 of gene PANK2 – heterozygous c.515_527del13 in exon 1b of gene PANK2 (p.Val172GlyfsX29) – heterozygous	1.5 T
P6	F, 14.2	c.1583C > T (p.Thr528Met) in exon 6 of gene PANK2 – heterozygous c.515_527del13 in exon 1b of gene PANK2 (p.Val172GlyfsX29) – heterozygous	1.5 T

[a]Reference sequence GenBank NM_153638.2.

Thus, a simple comparison based on routine PKAN genetic tests does not explain these differences, and probably some other factors are involved.

The present treatment of PKAN patients is, except for deep brain stimulation, based on the application of chelating agents that are able to cross the blood–brain barrier and accumulate iron ions. Iron ions in the brain are stored or released from ferritin, and changes in ferritin concentration correspond to changes of T_2 relaxivities in the globus pallidus. In pilot studies of PKAN treatment by deferiprone, no correlation between the decrease in T_2 relaxivities and clinical status was observed (19).

In our study, we have shown that there are at least two forms of iron as an intrinsic MR contrast agent with significantly different relaxivities, which contribute to the total relaxivity in the globus pallidus. Our two-compartment model demonstrates that the elimination of iron is a much more complicated process because chelates cannot eliminate iron microcrystals, and thus this type of treatment will probably be unsuccessful.

4. CONCLUSION

Our results obtained in PKAN patients showed a markedly decreased T_2 in the globus pallidus corresponding to high iron deposition. Based on investigations in different field strengths, we hypothesize that iron in the GP is present in at least two different forms. Besides the common physiological ferritin, a small portion of ferrimagnetic iron of unknown origin is present. Specifically, the total iron amount in the globus pallidus in PKAN patients in the form of ferritin is 99.7%, and 0.3% is in the form of SPIO. The proposed model explains why treatment with chelates has not been successful. A moderately increased T_2 in the putamen and nucleus caudatus in patients remains unexplained and requires further investigation.

Combination of *in vivo* relaxometry at MR systems working with different magnetic fields represents an interesting experimental tool for investigating the biophysical basis of various diseases.

5. SUBJECTS AND METHODS

5.1. Subjects

Six patients with genetically proven PKAN from five different families underwent MR imaging and relaxometry. Demographic and genetic data are summarized in Table 3. All six patients underwent an MR examination in a 1.5 T MR system. Two of them (patients P5 and P6) were later treated using deep brain stimulation because of their worsening clinical status, making further MR examination impossible (20). The remaining four patients were also measured in a 3 T whole-body system, and three of them underwent an additional examination in a 7 T whole-body system.

Control data were obtained from five healthy volunteers (three males, 41, 43 and 62 years old, and two females, 23 and 39 years old), who underwent examinations in all three magnetic fields. All controls and PKAN patients were informed about the examination protocol, and their (or their parents) written consent was obtained according to the local Ethical Committee rules.

5.2. MR examination

MR examinations were performed at three MR systems working in different magnetic fields: an 1.5 T Avanto equipped with a whole-body transmit and 12-channel receive head coil; a 3 T Tim Trio with a circularly polarized Helmholtz transmit/receive head coil; and 7 T Magnetom with a circularly polarized transmit/24-channel receive head coil (all Siemens Healthcare, Erlangen, Germany). T_2-weighted images in coronal, transversal and sagittal orientations were used for localization. For T_2 measurements we used a modified CPMG sequence with 32 echoes (echo-spacing *TE*, 6.9 ms; repetition time, *TR*, 3000 ms at 1.5 and 3 T; *TR* had to be prolonged to 5000 ms or more at 7 T owing to SAR limitation). T_2 relaxation times were measured in a 5 mm-thick tilted axial slice through the basal ganglia. The read out dimension of the field of view (anterior–posterior direction) was kept at 210 mm, while the dimension in the phase-encoding (left–right) direction varied from 161 to 187 mm according to the subject's anatomy. The voxel size was kept the same for each subject in all three magnetic fields. Each MR examination did not exceed 1 h in total.

T_2 maps were calculated in the whole slice using the home-made software ViDi described in Herynek *et al*. (21). Regions in the globus pallidus, putamen, caudate nucleus and frontal white matter in both hemispheres (Fig. 5) were selected and evaluated independently by three MR specialists. When the 'eye of the tiger' sign was visible, the dark rim and the hyperintense inner part of the GP were evaluated separately and the only dark rim area was used for further analysis. T_2 values were converted to

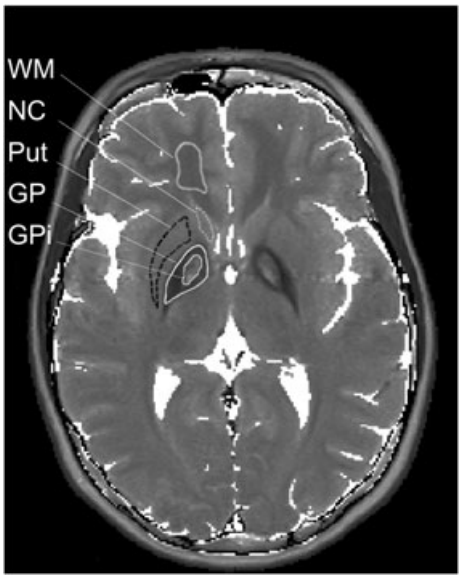

Figure 5. T_2 map of a PKAN patient with highlighted areas for T_2 value determination. WM, white matter; NC, nucleus caudatus; Put, putamen; GP, dark rim in the globus pallidus; GPi, hyperintense part of the globus pallidus.

reciprocal R_2 relaxation rates (i.e. $R_2 = 1/T_2$) for further analysis. Standard statistical tests (*F*-test, *t*-test) were used for the data analysis with a significance level of $p < 0.05$.

5.3. *In vitro* experiments

Phantoms (15 ml plastic tubes) containing different concentrations of ferritin (horse spleen ferritin, Sigma, CZ) and a SPIO-based contrast agent (Endorem®, Guerbet, France) suspended in 4% gelatine (gelatine from porcine skin, Sigma-Aldrich, Czech Republic) were prepared and measured in five different magnetic fields. The measurements at 1.5, 3 and 7 T were performed in the same MR systems using the same protocols as the human examinations. Echo time range and sampling were adjusted to the actual spin–spin relaxation. The examination was supplemented by measurements at 0.5 (Bruker MiniSpec 20 NMR analyzer; *TR*/*TE* = 5000/2 ms, number of echoes = 500) and 4.7 T (Bruker BioSpec 4.7/20 MR spectrometer; *TR*/*TE* = 5000/7.2 ms, number of echoes = 256; both systems Bruker Biospin, Ettlingen, Germany). The concentration of iron (*c*, μg/ml) in the samples was checked by atomic emission spectrometry. Relaxivities were calculated as reciprocal values of the relaxation time related to the iron concentration c (i.e. $r_2 = 1/T_2/c$).

5.4. Calculation of iron concentration in the brain

5.4.1. *One-component (ferritin only) model*

The iron concentration in the globus pallidus was calculated using the following empirical equation derived in Hajek *et al.* (13) for 1.5 T measurement:

$$c_{Fe} = 37/T_2 - 358 \quad (1)$$

where T_2 is the measured relaxation time (in s) and c_{Fe} is the iron concentration (μg/ml). The equation was derived from the age dependence of the iron content (1) and T_2 relaxation times (14) obtained at 1.5 T. The equation assumes that iron is accumulated in the form of ferritin only (14,22,23).

5.4.2. *Two-component (ferritin and superpamaramagnetic iron) model*

This model is based on the assumption that surplus iron is stored both in the form of antiferromagnetic ferritin and also in a ferrimagnetic form. The contribution of the surplus iron to the R_2 relaxation rate was estimated as the difference ΔR_2 between the patients' and controls' relaxation rates. To determine the two components of the deposited iron, the field-dependent contribution ΔR_2 was then evaluated as the linear combination of the experimentally determined ferritin and ferrimagnetic iron relaxivities using a least-square analysis.

Acknowledgments

The authors would like to acknowledge the willingness of the PKAN patients and their parents and also their medical staff, who enabled us to contact them. The study was financially supported by the following grants: Internal Grant Agency of the Ministry of Health, Czech Republic, no.10523-3; Ministry of Health, Czech Republic, Institutional support 00023001; Program AKTION, Czech Republic-Austria, no. 56p22.

REFERENCES

1. Hallgren B, Sourander P. The effect of age on the non-haemin iron in the human brain. J Neurochem 1958; 3: 41–51.
2. Gregory A, Hayflick SJ. Pantothenate kinase-associated neurodegeneration. In GeneReviews, Pagon RA, Bird TD, Dolan CR, Stephens K (eds) [Internet]. University of Washington, Seattle: Seattle, WA; 1993–2002 [updated 2010 Mar 23]. http://www.ncbi.nlm.nih.gov/books/NBK1490/
3. Delgado RF, Sanchez PR, Speckter H, Then EP, Jimenez R, Oviedo J, Dellani PR, Foerster B, Stoeter P. Missense PANK2 mutation without 'eye of the tiger' sign: MR findings in a large group of patients with pantothenate kinase-associated neurodegeneration (PKAN). J Magn Reson Imag 2012; 35: 788–794.
4. Huang J, Zhong X, Wang L, Yang L, Mao H. Improving the magnetic resonance imaging contrast and detection methods with engineered magnetic nanoparticles. Theranostics 2012; 2(1): 86–102.
5. Vymazal J, Zak O, Bulte JW, Aisen P, Brooks RA. T_1 and T_2 of ferritin solutions: effect of loading factor. Magn Reson Med 1996; 36: 61–65.
6. Gossuin Y, Muller RN, Gillis P. Relaxation induced by ferritin: a better understanding for an improved MRI iron quantification. NMR Biomed 2004; 17: 427–432.
7. Gossuin Y, Roch A, Muller RN, Gillis P. Relaxation Induced by ferritin and ferritin-like magnetic particles: the role of proton exchange. Magn Reson Med 2000; 43: 237–243.
8. Hocq A, Brouette N, Saussez S, Luhmer M, Gillis P, Gossuin Y. Variable-field relaxometry of iron-containing human tissues: a preliminary study. Contrast Media Mol Imag 2009; 4(4): 157–164.
9. Brooks RA, Vymazal J, Goldfarb RB, Bulte JWM, Aisen P. Relaxometry and magnetometry of ferritin. Magn Reson Med 1998; 40(2): 227–235.
10. Hallervorden J, Spatz H. Peculiar disease in the extrapyramidal system with particular consideration for the globus pallidus and the substantia nigra – an article on the connections between these two centres. [Ger] Z Gesamte Neurol Psychiatr 1922; 79: 254–302.
11. Weissleder R, Stark DD, Engelstad BL, Bacon BR, Compton CC, White DL, Jacobs P, Lewis J. Superparamagnetic iron oxide: pharmacokinetics and toxicity. Am J Roentgenol 1989; 152(1): 167–173.
12. Saudek F, Jirak D, Girman P, Herynek V, Dezortova M, Kriz J, Peregrin J, Berkova Z, Zacharovova K, Hajek M. Magnetic resonance imaging of pancreatic islets transplanted into the liver in humans. Transplantation 2010; 90(12): 1602–1606.
13. Hajek M, Adamovicova M, Herynek V, Skoch A, Jiru F, Krepelova A, Dezortova M. MR relaxometry and 1H MR spectroscopy for the determination of iron and metabolite concentrations in PKAN patients. Eur Radiol 2005; 15(5): 1060–1068.
14. Schenker C, Meier D, Wichmann W, Boesiger P, Valavanis A. Age distribution and iron dependency of the T_2-relaxation time

in the globus-pallidus and putamen. Neuroradiology 1993; 35(2): 119–124.
15. Gossuin Y, Burtea C, Monseux A, Toubeau G, Roch A, Muller RN, et al. Ferritin-induced relaxation in tissues: an *in vitro* study. J Magn Reson Imag 2004; 20: 690–696.
16. Swaiman KF. Hallervorden–Spatz Syndrome and brain iron-metabolism. Arch Neurol 1991; 48(12): 1285–1293.
17. Dobson J. Nanoscale biogenic iron oxides and neurodegenerative disease. FEBS Lett 2001; 496(1): 1–5.
18. Perry TL, Norman MG, Yong VW, Whiting S, Crichton JU, Hansen S, Kish SJ. Hallervorden–Spatz disease: cysteine accumulation and cysteine dioxygenase deficiency in the globus pallidus. Ann Neurol 1985; 18: 482–489.
19. Zorzi G, Zibordi F, Chiapparini L, Bertini E, Russo L, Piga A, Longo F, Garavaglia B, Aquino D, Savoiardo M, Solari A, Nardocci N. Iron-related MRI images in patients with pantothenate kinase-associated neurodegeneration (PKAN) treated with deferiprone: results of a phase II pilot trial. Mov Dis 2011; 26(9): 1756–1759.
20. Adamovicova M, Urgosik D, Spackova N, Krepelova A. Pallidal stimulation in siblings with pantothenate kinase-associated neurodegeneration: four-year follow-up. Mov Disord 2011; 26(1): 184–187.
21. Herynek V, Wagnerova D, Hejlova I, Dezortova M, Hajek M. Changes in the brain during long-term follow-up after liver transplantation. J Magn Reson Imag 2012; 35: 1332–1337.
22. Vymazal J, Brooks RA, Patronas N, Hajek M, Bulte JWM, DiChiro G. Magnetic resonance imaging of brain iron in health and disease. J Neurol Sci 1995; 134(Suppl S): 19–26.
23. Vymazal J, Brooks RA, Baumgarner C, Tran V, Katz D, Bulte JWM, Bauminger ER, DiChiro G. The relation between brain iron and NMR relaxation times: an *in vitro* study. Magn Reson Med 1996; 35(1): 56–61.

